JOURNAL OF GEOPHYSICAL RESEARCH, VOL. 91, NO. D1, PAGES 1073–1088, JANUARY 20, 1986

The H_2SO_4-HNO_3-NH_3 System at High Humidities and in Fogs 1. Spatial and Temporal Patterns in the San Joaquin Valley of California

DANIEL J. JACOB,[1] J. WILLIAM MUNGER, JED M. WALDMAN, AND MICHAEL R. HOFFMANN

Environmental Engineering Science, W. M. Keck Engineering Laboratories, California Institute of Techology, Pasadena

A systematic characterization of the atmospheric H_2SO_4-HNO_3-NH_3 system was conducted in the fog water, the aerosol, and the gas phase at a network of sites in the San Joaquin Valley of California. Spatial patterns of concentrations were established that reflect the distribution of SO_2, NO_x, and NH_3 emissions within the valley. The concept of atmospheric alkalinity was introduced to interpret these concentrations in terms of the buffering capacity of the atmosphere with respect to inputs of strong acids. Regions of predominantly acidic and alkaline fog water were identified. Fog water was found to be alkaline in most of the valley, but small changes in emission budgets could lead to widespread acid fog. An extended stagnation episode was studied in detail: progressive accumulation of H_2SO_4-HNO_3-NH_3 species was documented over the course of the episode and interpreted in terms of production and removal mechanisms. Secondary production of strong acids H_2SO_4 and HNO_3 under stagnant conditions resulted in a complete titration of available alkalinity at the sites farthest from NH_3 sources. A steady SO_2 conversion rate of 0.4–1.1% h^{-1} was estimated in the stagnant mixed layer under overcast conditions and was attributed to nonphotochemical heterogeneous processes. Removal of SO_2 was enhanced in fog, compared to nonfoggy conditions. Conversion of NO_x to HNO_3 slowed down during the stagnation episode because of reduced photochemical activity; fog did not appear to enhance conversion of NO_x. Decreases in total HNO_3 concentrations were observed upon acidification of the atmosphere and were attributed to displacement of NO_3^- by H_2SO_4 in the aerosol, followed by rapid deposition of HNO_3(g). The occurrence of fog was associated with general decreases of aerosol concentrations due to enhanced removal by deposition.

INTRODUCTION

Extremely high acidities have been reported in fogs and low stratus clouds collected in southern California [*Munger et al.*, 1983; *Brewer et al.*, 1983; *Waldman et al.*, 1985; *Jacob et al.*, 1984*a*, 1985]. The acidity of these fogs was due to H_2SO_4 and HNO_3, while NH_3 was found to be the main alkaline species titrating the acidity [*Jacob et al.*, 1984*a*]. Therefore one can attempt to model the "acid fog" phenomenon by consideration of acid-base neutralization processes in the H_2SO_4-HNO_3-NH_3 atmospheric system.

Ammonia is released directly to the atmosphere from a variety of sources [*Cass et al.*, 1982], but H_2SO_4 and HNO_3 are mostly produced by atmospheric oxidation of reduced sulfur and nitrogen compounds. Oxidation of SO_2 to H_2SO_4 proceeds in the gas phase [*Calvert and Stockwell*, 1984], in concentrated aerosol [*Kaplan et al.*, 1981; *Crump et al.*, 1983], and in dilute aqueous solutions [*Martin*, 1984]. Oxidation of NO_x to HNO_3 proceeds in the gas phase by the reaction $NO_2 + OH$ and may also proceed heterogeneously following scavenging by aerosol of NO_3 and N_2O_5 produced from the reaction $NO_2 + O_3$ [*Heikes and Thompson*, 1983]. Nitrite is slowly oxidized to NO_3^- in dilute solutions [*Damschen and Martin*, 1983]. Using data available for S(IV) and N(III) oxidation reactions, *Jacob and Hoffmann* [1983] predicted that aqueous phase oxidation of S(IV) in fog droplets could be an important source of H_2SO_4 under polluted conditions; on the other hand, they found that aqueous phase oxidation of N(III) provided only a very small source of HNO_3.

Sulfuric acid is present as an aerosol under usual atmospheric conditions, but HNO_3 and NH_3 have substantial vapor pressures over ammonium nitrate aerosol [*Stelson and Seinfeld*, 1982]. The atmospheric residence times of HNO_3 and NH_3 are strongly dependent on their partitioning between the gas phase and the aerosol. The gaseous species are quickly removed by deposition (1–5 cm s^{-1} for HNO_3(g) over grass [*Huebert*, 1983]). On the other hand, secondary particles formed from H_2SO_4-HNO_3-NH_3-H_2O mixtures are typically in the size range 0.1–1 μm and have low deposition velocities of the order of 0.01–0.1 cm s^{-1} [*Sehmel*, 1980; *Slinn*, 1982]. The occurrence of fog enhances the removal of aerosol species because growth of particles to fog droplet size considerably increases their deposition rates. Fog droplet deposition velocities of 2–7 cm s^{-1} over short grass [*Dollard and Unsworth*, 1983] and 2–4 cm s^{-1} over a dirt surface [*Waldman*, 1986] have been reported.

A general mechanism to account for fog water acidity in polluted atmospheres may therefore include six fundamental processes: (1) emissions of SO_2, NO_x, and NH_3, (2) pollutant transport, (3) secondary production of H_2SO_4 and HNO_3, (4) detailed chemical speciation within the H_2SO_4-HNO_3-NH_3-H_2O system, (5) scavenging by fog droplets, and (6) in-fog aqueous phase oxidation of reduced N and S species.

The San Joaquin Valley of California is an excellent "field laboratory" for the interpretation of fog water composition in terms of the above processes. It is the site of major oil recovery operations, which release large amounts of SO_2 and NO_x. In addition, agricultural and livestock-feeding activities provide important sources of NH_3. Severe stagnation episodes, associated with persistent fog and low-lying stratus clouds, occur frequently during the winter months. These stagnation episodes are caused by persistent temperature inversions based a few hundred meters above the valley floor and below the surrounding mountain ridges [*Holets and Swanson*, 1981]. Tracer studies have documented the lack of ventilation in the valley during these prolonged episodes [*Reible*, 1982]

In a preliminary study at a single site from December 1982 to January 1983, *Jacob et al.* [1984*a*] documented the main

[1]Now at Center for Earth and Planetary Physics, Harvard University, Cambridge, Massachusetts.

Paper number 5D0727.
0148-0227/86/005D-0727$05.00

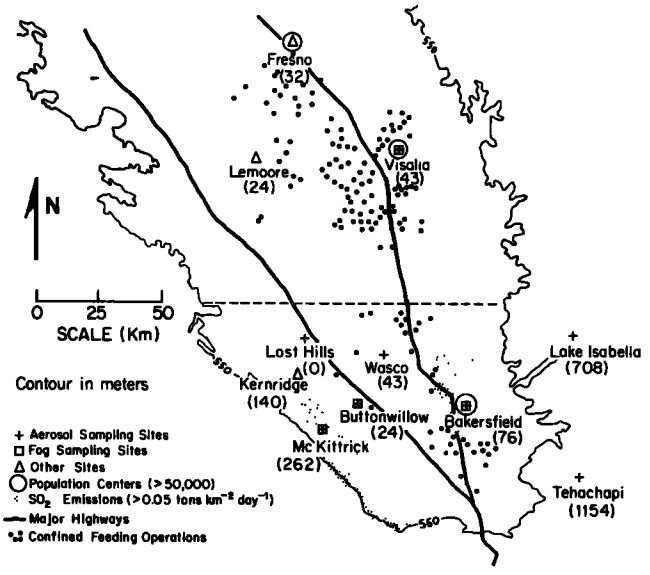

Fig. 1. Sampling sites in the San Joaquin Valley of California. Important emission sources (oil fields, major highways, confined feeding operations) are indicated. The dashed line is the Kern County line, which is the northern boundary of the area referred to in the text as the "southern San Joaquin Valley" (SSJV). Elevations in meters are given for each site, based on a reference elevation at Lost Hills, the lowest site (57 m above mean sea level).

features of aerosol and fog water chemical composition during stagnation episodes in the San Joaquin Valley. The main features observed were as follows: (1) important accumulation of secondary aerosol proceeded under nonfoggy but stagnant conditions, (2) significant pollutant deposition occurred over the course of fog events, (3) SO_2 conversion in fogs did not exceed a few percent per hour, and (4) the fog water *pH* was determined by the availability of NH_3 to neutralize the H_2SO_4 and HNO_3 present.

A more comprehensive study was conducted during January 1984, of which this report presents the main results. Aerosol, fog water, and gas phase concentrations were monitored at a network of sites. Spatial and temporal variations of atmospheric concentrations are established that reflect both the geographical distribution of emission sources and the meteorological conditions. The concept of atmospheric alkalinity is introduced to predict the potential for high-acidity fog events. Pollutant accumulation and removal over the course of a stagnation episode are characterized under both foggy and nonfoggy conditions. The rate of oxidation of SO_2 to H_2SO_4 is estimated. The effect of stagnation on HNO_3 production is discussed. The partitioning of the H_2SO_4-HNO_3-NH_3 system between the gas phase, the aerosol, and the fog water is interpreted in a companion paper in terms of a thermodynamic model [*Jacob et al.*, this issue]. The complete fog water, aerosol, and gas phase data set is given by *Jacob* [1985].

EXPERIMENTAL

The volumetric concentrations of aerosol, HNO_3(g), and NH_3(g) were monitored at eight sites over the period December 31, 1983, to January 14, 1984 (Figure 1). Samples were collected twice daily (0000–0400 and 1200–1600 PST) at the six valley sites and once daily (1000–1600 PST) at the two mountain sites (Tehachapi and Lake Isabella). The sampling stations were located on platforms 15 m above the ground (Wasco and Tehachapi), on the roof of a building or trailer (Bakersfield, Lost Hills, Buttonwillow, McKittrick, and Visalia), or on the ground, 1.5 m above a grassy area (Lake Isabella). Two open-faced 47-mm Gelman Zefluor Teflon filters (1-μm pore size) were operated side by side (10 L min^{-1}) to provide duplicate determinations of the inorganic content of the aerosol. A flat cover 15 cm above the filters prevented collection of large particles by sedimentation. The Stokes number at the filter inlet is 0.05 for a 50-μm-diameter particle, so that even very large fog droplets should be efficiently sampled [*Davies and Subari*, 1982]. Under foggy conditions the determinations of total aerosol NO_3^- and NH_4^+ may be subject to errors because of evaporative losses (see the appendix), and those numbers subject to error were excluded from the data interpretation. A 47-mm Gelman Nylasorb nylon filter collected gaseous nitric acid immediately downstream of one of the Teflon filters, and an oxalic-acid-impregnated glass fiber filter collected gaseous ammonia immediately downstream of the other Teflon filter.

The filters were sealed in petri dishes and kept at 4°C following collection. The Teflon filters were extracted in 10 mL of distilled deionized water (Corning Megapure) for 90 min, using a reciprocating shaker; complete extraction was indicated by insignificant concentrations in repeated extractions. The extracts were analyzed for major ions using standard methods previously described by *Munger et al.* [1983]. The nylon filters were extracted for 90 min, using a reciprocating shaker in a solution 3 m*M* HCO_3^- and 2.4 m*M* CO_3^{2-} (a conventional ion chromatography eluent). Oxalic-acid-impregnated filters were extracted and analyzed following the protocol of *Russell* [1983]. Ion chromatography revealed low levels of S(IV) in the Teflon filter extracts, but these concentrations were small compared to SO_4^{2-}, and their contributions were ignored. Although most of the aerosol sulfur is expected to be present as SO_4^{2-}, some of the measured SO_4^{2-} may have resulted from the oxidation of reduced sulfur species on the filter or in the extract.

Fogs were sampled by event at four sites (Figure 1). Fog water samples were collected with a rotating arm collector [*Jacob et al.*, 1984*b*] for intervals ranging from 30 min to 3 hours. The rotating arm collector has a theoretical sampling rate of 5 m^3 min^{-1} and has been shown to collect fog water samples without evaporation or condensation. Laboratory calibration has indicated a lower size cut (50% collection efficiency) of 20-μm diameter. Because the instrument collects fog droplets by direct impaction and does not require drawing air through an inlet, large fog droplets are efficiently collected. Liquid water content in the fog was determined from the sampling rate of the instrument, assuming that 60% of the total liquid water sampled was actually collected [*Waldman*, 1986].

Fog water samples were preserved and analyzed for major ions and trace metals following the protocol described by *Munger et al.* [1983], with the exception described below. In fog water samples, significant S(IV) concentrations are found during conventional anion analysis by ion chromatography. A possible explanation is the formation of stable but reversible S(IV)-*R*CHO adducts, such as $CH_2(OH)SO_3^-$ [*Munger et al.*, 1984]. The standard ion chromatographic method (Dionex AS-3 column, [3 m*M* HCO_3^- + 2.4 m*M* CO_3^{2-}] eluent, 3 mL min^{-1} flow rate) proposed by *Dionex Corporation* [1981] and used by *Munger et al.* [1983] does not clearly separate S(IV) and NO_3^-. Better separation is achieved with a weaker eluent or with the Dionex AS-4 column, but quantification of S(IV) remains unsatisfactory. To solve this problem, aliquots for anion determination were spiked to 0.09 *M* H_2O_2 several minutes prior to injection and simultaneously made alkaline

by the usual addition of HCO_3^- and CO_3^{2-} to match the eluent; this procedure was found to result in the quantitative oxidation of HSO_3^- and $CH_2(OH)SO_3^-$ standards to SO_4^{2-} and the total suppression of the S(IV) peak in fog water samples. Sulfur(IV) concentrations were separately determined by a pararosaniline colorimetric method on aliquots preserved with buffered (*p*H 4) CH_2O immediately upon sample collection [*Dasgupta et al.*, 1980]. Fog water SO_4^{2-} concentrations were calculated by subtracting the S(IV) concentrations thus obtained from the SO_4^{2-} concentrations determined by ion chromatography. Concentrations of carboxylate ions were determined by ion exclusion chromatography [*Keene et al.*, 1983].

To date there are no standardized sampling procedures for the collection of fog water and aerosol samples for chemical analysis. Therefore it is important to assess the errors associated with our methods. A detailed discussion of sampling biases, artifacts, and standard errors on our data is presented in the appendix.

Hourly average concentrations of SO_2 were measured at Bakersfield by the Getty Oil Company and at McKittrick, Kernridge, and Lost Hills by West Side Operators (WSO). Concentrations of nitrogen oxides, CO, and O_3 were monitored at Kernridge by WSO. Surface winds were measured by WSO (Lost Hills, Kernridge, McKittrick, and Maricopa), Getty Oil Company (Bakersfield), National Weather Service (NWS) (Bakersfield and Fresno), Lemoore Naval Air Force Base, and Kern County Fire Department (Tehachapi). Upper level winds were measured at Edwards Air Force Base, located in the Mojave Desert on the SE side of the Tehachapi Mountains. Mixing heights were measured hourly by WSO at Kernridge with an acoustic sounder. Additional weather data were available from the National Weather Service station at Bakersfield.

To account for the equilibria between gas and aerosol phases, we define S(VI), N(V), and N(−III) to represent the element at the given oxidation state, both in the gas and aerosol phases. Thus N(V) includes HNO_3(g) and NO_3^-, and N(−III) includes NH_3(g) and NH_4^+. We further define [*A*] as the concentration of constituent *A* in fog water (moles per liter of water), and (*A*) as the concentration of *A* in air (moles per cubic meter of air). Concentrations of HNO_3(g) will generally be given in equivalents, for consistency with the units of NO_3^- and NH_4^+ concentrations. "Equivalent" in that sense refers to the proton donor/acceptor capacity of the gas when scavenged by the aerosol. Both HNO_3(g) and NH_3(g) contribute one equivalent per mole; 1 ppb = 43 neq m^{-3} at 5°C.

WEATHER PATTERN AND POLLUTANT TRANSPORT

Figure 2 shows the profile versus time of mixing heights and stratus cloud bases over the valley floor during the sampling program. Two types of mixing height diurnal patterns were observed.

In the first pattern (December 31 to January 1, January 10–12, and January 14), ground-based inversions formed by radiation at night and broke up the following afternoon, leading to mixing heights in excess of 1000 m above ground level (AGL). This pattern was usually associated with clear skies or high cloudiness, but fogs in ground-based inversions were occasional occurrences (for example, at Bakersfield on December 31). Figure 3*a* gives the average wind vectors on the days when this pattern was observed. A net slow NW flow was observed on the valley floor, and upper level winds were NW; this is the usual flow in the area and reflects the circulation around the Pacific High off the California coast. Terrain influences in the southern end of the valley led to convergence of the flow in the SE corner of the valley. Surface winds in the valley frequently shifted in direction, and erratic low winds were typically observed under nighttime stable conditions.

Concentrations of trace gases at Kernridge were lowest on the days when this first pattern was observed (Figure 2) and so were aerosol concentrations [*Jacob*, 1985]. Because net horizontal transport was very slow (Figure 3*a*), it is unlikely that surface winds ventilated the valley by transport over the mountain ridges in the SE corner of the valley. Aerosol concentrations at Tehachapi and Lake Isabella remained much lower than in the valley, which is evidence against such transport. Instead, pollutant removal was due to rapid vertical mixing as the inversion broke up in the afternoon; this vertical mixing diluted the polluted air parcels and allowed their rapid transport by strong upper level NW winds to the surrounding air basins.

A different mixing height pattern was observed on January 2–7; during that period a strong temperature inversion based a few hundred meters above the ground persisted over the valley. This inversion was due to mesoscale subsidence associated with a stationary high-pressure system (Great Basin High) centered over southern Idaho and northern Nevada. Upper level winds at Edwards Air Force Base switched from NW to east during that period (circulation around the Great Basin High), and afternoon winds at Tehachapi were SE. The valley was capped throughout the January 2–7 period by a stratus cloud filling the upper part of the mixed layer (Figure 2); this cloud frequently intercepted the McKittrick site 250 m above the valley floor. On the night of January 4–5 the stratus base lowered sufficiently to cause fog at elevated sites on the valley floor (Kernridge and Bakersfield NWS station), although most of the valley floor remained overcast. On the nights of January 5–6 and 6–7 the stratus base lowered sufficiently to fill the entire mixed layer, as shown in Figure 2, and dense fog was observed throughout the valley. The cloud layer then deepened considerably on January 7–8; mixing heights rose to above 1000 m AGL, and drizzle fell on the valley floor. On January 9 the inversion base dropped again, but upper level winds had switched back to NW. After January 10 the first mixing height pattern (surface inversions at night breaking up in the afternoon) was again observed.

The capping of the valley by a persistent inversion based at a lower altitude than the surrounding mountain ridges obviously restricted ventilation. Concentrations of trace gases at Kernridge (Figure 2) increased over the stagnant January 2–7 period and dropped on January 8, when the mixing height rose above the mountain ridges. Concentrations then increased again on January 9–10 and dropped on January 10.

Winds in the valley during the January 2–7 period are shown in Figure 3*b*. Net horizontal transport was extremely slow. Cross-valley winds were dominant south of Lost Hills; farther north, however, a net flow north out the valley was observed. *Reible* [1982] had previously observed similar flow patterns during stagnation episodes in the valley and found pollutant transport in the southern end of the valley to be extremely complex because of the upslope flow/downslope flow systems associated with the mountain/valley breezes. He concluded from a series of tracer releases that the southern San Joaquin Valley behaved as a stirred tank with a mixing time of 1–2 days, slowly ventilated by the outflow at its northern end. We will try to interpret our data in term of that simple model, and for that purpose we define the "southern San Joaquin Valley" (SSJV) as that portion of the valley south of the Kern County line (see Figure 1).

Figure 3*b* indicates a zone of inflow along the western edge of the SSJV and two possible outflows to the north and to the

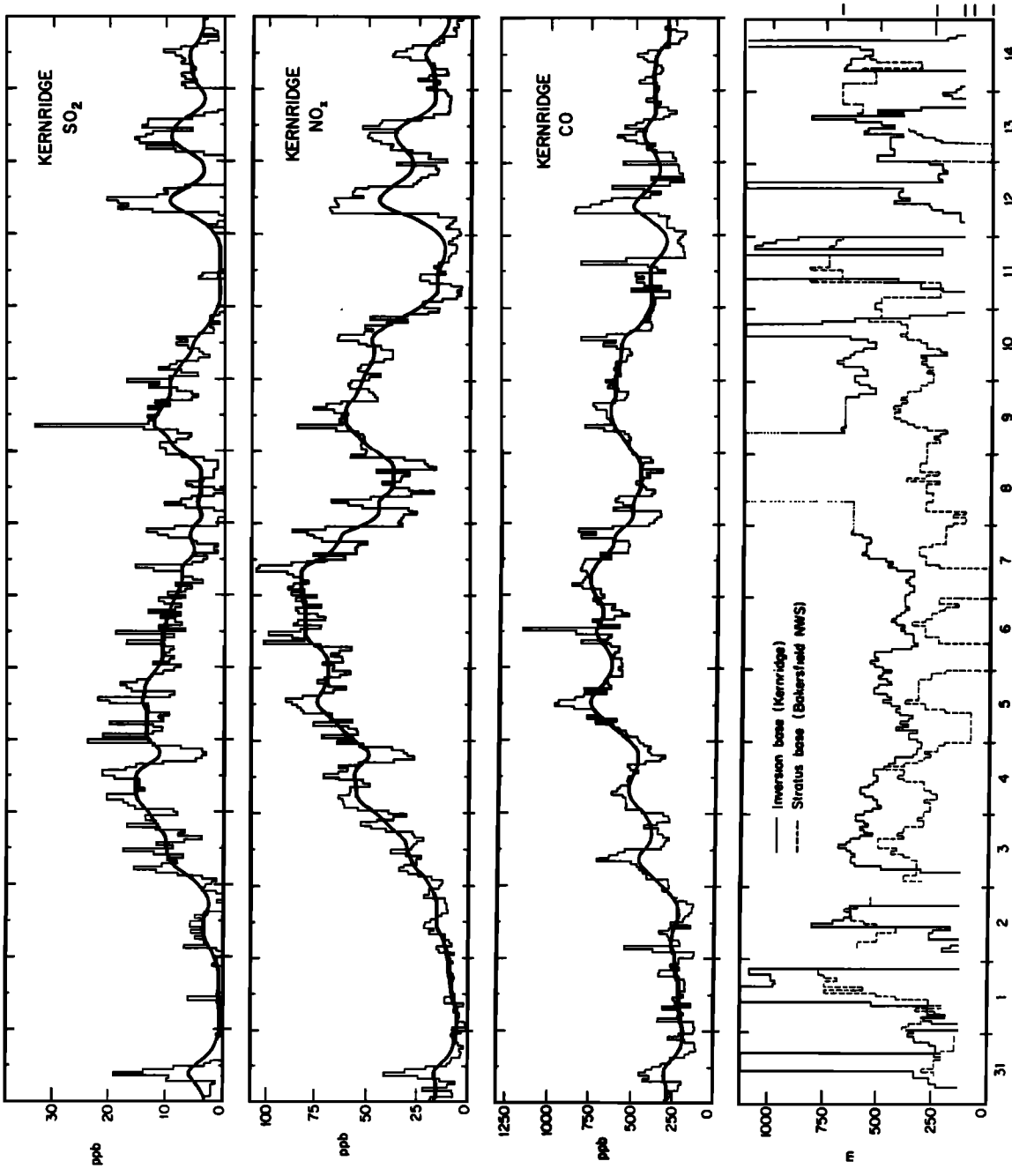

Fig. 2. Concentrations of SO_2, NO_2, and CO at Kernridge: the bold lines were obtained by smoothing the data with a digital filter. Also given are mixing heights (stratus cloud tops) measured at Kernridge and stratus cloud bases measured at the Bakersfield National Weather Service station. The reference altitude is that at Lost Hills, the lowest site on the valley floor. Kernridge hourly mixing height data were missing for January 8–9 (dotted line in the mixing height profile), and mixing heights for that period were interpolated from scattered measurements at Kernridge and cloud top data from pilot reports. Discontinuities in the mixing height profile at the altitude of Kernridge indicate a surface inversion at Kernridge. Discontinuities in the mixing height profile at 1000 m AGL indicate a mixing height in excess of 1000 m AGL.

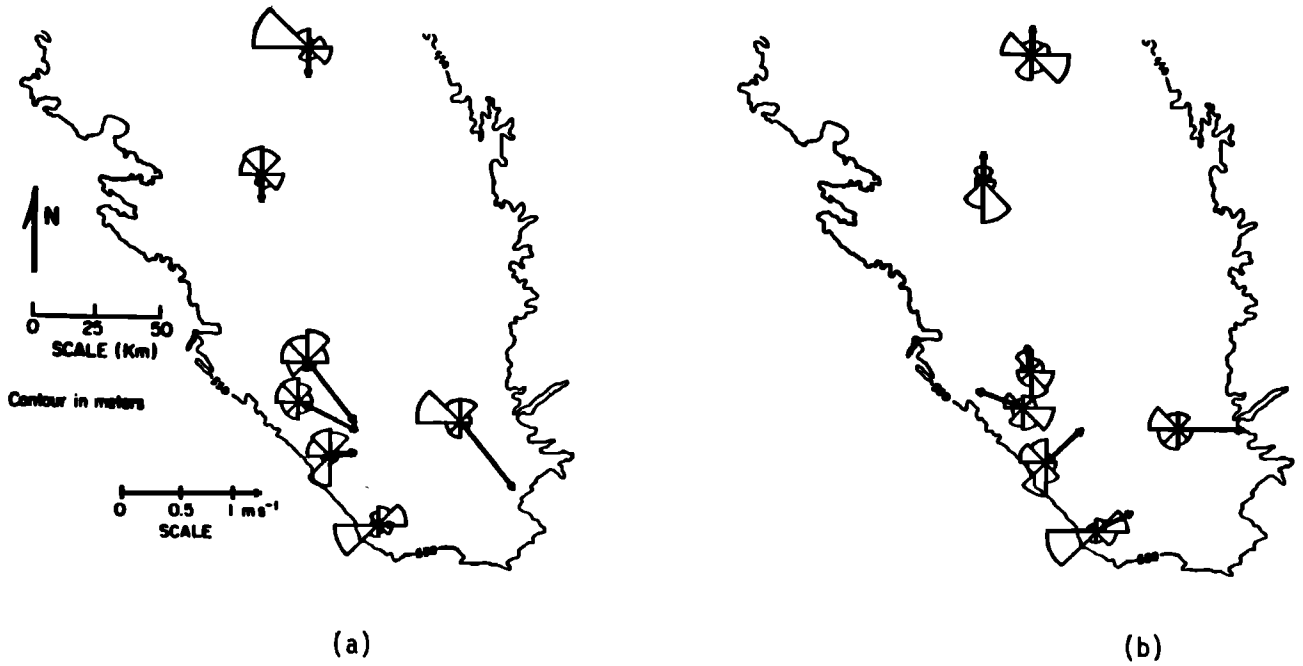

Fig. 3. Flow patterns during the sampling program. The wind roses indicate the frequencies of wind directions. The wind vector is the resultant wind (calculated by averaging the hourly wind vectors). (*a*) Nonstagnant conditions (December 31 to January 1, January 11–12, January 14). (*b*) Stagnant conditions (January 2–7).

east. However, very little transport of boundary layer air is expected over the mountain ridges on the eastern edge of the valley. The inversion did not break down or lift near the slopes: the stratus cloud intercepted the Bakersfield-Tehachapi highway as a well-defined fog layer, and the community of Tehachapi always remained sunny and clear. Further, winds in the SSJV were entirely decoupled from the circulation aloft, as indicated by the upper level winds to the east at Edwards AFB and the SE winds at Tehachapi. Aerosol concentrations remained very low at Tehachapi and Lake Isabella throughout the episode.

Therefore slow transport north out of the valley was the main outflow for SSJV air. Resultant winds at Lemoore, Fresno, and Lost Hills were consistent (Figure 3*b*). Projections of these winds on the valley axis (150°) yielded average speeds of 0.24, 0.26, and 0.22 m s^{-1} at each site, respectively. Since the SSJV is about 100 km long, this flow led to an average residence time of 5 days for an air parcel within the SSJV. The accumulation pattern for CO at Kernridge (Figure 2) suggests approach of a steady state by January 5, which is consistent with a residence time of 5 days.

AVERAGE S(VI), N(V), AND N(−III) CONCENTRATIONS AT EACH SITE

The SSJV is the site of important SO_2, NO_x, and NH_3 emissions (Table 1). The geographical distribution of the main emission sources is shown in Figure 1. Most of the NH_3 is emitted from confined-feeding operations concentrated on the east side of the valley, especially around Bakersfield and Visalia. Another important source of NH_3 is cropland, which occupies most of the land in the valley floor not used for oil recovery operations, and the associated fertilizer use. Emissions of SO_2 and NO_x are concentrated in the east side and west side oil fields of the SSJV; the oil field emissions originate mostly from small boilers, which release their exhausts 10–20 m above the ground and therefore affect the immediate surroundings. Mobile sources (two major highways, off-road farm equipment, and city traffic) also contribute to NO_x emissions.

Spatial patterns of aerosol and fog water concentrations (Tables 2 and 3*a*–3*c*) directly reflected the distribution of emission sources. The ionic content of aerosol in the valley was dominated by SO_4^{2-}, NO_3^-, and NH_4^+, which typically contributed over 90% of the total measured ionic loading. Concentrations of N(−III) were highest at Bakersfield and Visalia, near the large cattle feedlots, and lowest on the west side (Lost Hills and McKittrick). Mountain sites (Lake Isabella and Tehachapi), which have no important local NH_3 sources, had very low N(−III) concentrations.

Concentrations of S(VI) were highest at Bakersfield, which is within the east side oil fields; they were also high at McKittrick, which is within the west side oil fields, and at Buttonwillow, directly downwind of the west side oil fields. Concentrations of S(VI) at Wasco, Lost Hills, and Visalia were lower, reflecting their respective distances from oil recovery operations. Concentrations of S(VI) at the two mountain sites were very low and indicated no observable impact from the valley air.

Because most of the NO_x was emitted from the same sources as SO_2, one would expect the spatial distribution of N(V) concentrations to be similar to that of S(VI). Indeed, N(V) concentrations were highest at Bakersfield; however, N(V) concentrations at McKittrick were low. The lack of NH_3 at McKittrick frequently led to acidic conditions, in which N(V) would be mostly present as HNO_3(g) and therefore quickly removed by deposition. This point will be addressed in more detail below. Concentrations of N(V) were higher at Visalia than would be expected from the spatial distribution of S(VI); Visalia is an important population center, and emissions from mobile sources were probably the dominant source of N(V) precursors at that site.

Fog water concentrations of trace metals were consistent with the above analysis (Table 3*b*). Concentrations of Ni and V, which are almost exclusively associated with residual oil burning [*Cooper and Watson*, 1980], were high at Bakersfield,

TABLE 1. SO_2, NO_x, and NH_3 Emission Inventories for the Southern San Joaquin Valley

Source	Emissions, t d^{-1}
SO_2[a]	
Oil production	
east side	116
west side	69
Agriculture	1
Mobile sources	6
Total emissions	1972
NO_x[b]	
Stationary sources[c]	138
Mobile sources	52
Total emissions	190
NH_3[d]	
Livestock	46
Soil	18
Fertilizer use	10
Domestic	3
Fuel combustion	2
Total emissions	79

See Figure 1 for definition of southern San Joaquin Valley. Area is 7930 km^2.

[a] *Aerovironment, Incorporated* [1984], December 1982 data.

[b] *California Air Resources Board* [1982], 1979 data.

[c] Mostly oil and gas production.

[d] *Jacob* [1985], January 1984 data.

McKittrick, and Buttonwillow and low at Visalia. Concentrations of Pb, which is emitted by automobile exhaust, were high in the population centers (Bakersfield and Visalia) and low at rural sites (McKittrick and Buttonwillow).

Overall, the large differences in S(VI), N(V), and N(−III) concentrations that were observed from one site to another over distances of only a few tens of kilometers show that the composition of the H_2SO_4-HNO_3-NH_3 system at each site was strongly determined by the nature of emission sources in the immediate vicinity. A chemical balance on primary aerosol (based on the work by *Cooper and Watson* [1980]) indicated that all but a negligible fraction of the total S(VI) in the valley was of secondary origin. However, in spite of the time required for oxidation of SO_2 to H_2SO_4, the areas of SO_2 emissions matched the areas of high S(VI) concentrations. This supports our observation that horizontal pollutant transport on the valley floor was very slow. Under such conditions, fog water acidity should be directly determined by the relative abundances of local acidic (SO_2, NO_x) and alkaline (NH_3) emissions. Indeed, Table 3 indicates that fog water acidity differed greatly from site to site, depending on the availability of NH_3 to neutralize S(VI) and N(V); low *p*H values were found at McKittrick and very high *p*H values were found at Visalia. The *p*H of fog samples collected simultaneously at four sites during the widespread January 7 fog event clearly showed this spatial pattern (Figure 4). Acidic fog was consistently observed at McKittrick but never at the other sites.

Acidic fog had frequently been observed at the Bakersfield site during the previous winter [*Jacob et al.*, 1984*a*]. In view of the close balance of acids and bases at that site, small fluctuations in emissions can result in a lack of available base to titrate acid inputs. To predict the vulnerability of an atmosphere to an "acid fog" problem, one must have a quantitative measure of the acid-neutralizing capacity of that atmosphere. To this end we now introduce the concept of atmospheric alkalinity, defined by analogy to the concept of alkalinity used in the aquatic chemistry literature [*Stumm and Morgan*, 1970].

ATMOSPHERIC ALKALINITY

We define fog water alkalinity [ALK] as the deficiency of aqueous phase H^+ with respect to the reference system of "neutralized" fog water species (CAT^{n+}, Cl^-, NO_3^-, SO_4^{2-}, $S(IV)^-$, CO_2, *HA*). CAT^{n+} refers to cations other than H^+, and *HA* refers to undissociated weak acids other than CO_2. In the *p*H range 3–8 the following expression for [ALK] can be used to a good approximation:

$$[ALK] = \sum [A^-] + [S(IV)^{2-}] + [HCO_3^-] + [NH_3(aq)] + [OH^-] - [H^+] \quad (1)$$

The main S(IV) species in the *p*H range 2–7 are expected to be HSO_3^- and stable monovalent S(IV) adducts [*Jacob and Hoffmann*, 1983; *Munger et al.*, 1984; *Boyce and Hoffmann*, 1984]. Therefore the monovalent form of S(IV) is most appropriate for use as reference. If CO_2 was the only weak acid present, fog water at the reference point ([ALK] = 0) would correspond to pure water in equilibrium with atmospheric CO_2, and the corresponding reference *p*H would be about 5.6; because additional weak acids are present, the reference *p*H is lower. At the concentrations of carboxylic acids found in the San Joaquin Valley (Table 2) the reference *p*H is of the order of 4.5. This is still above the threshold at which environmental damage from "acid fog" may be anticipated [*Scherbatskoy and Klein*, 1983; *Granett and Musselman*, 1984; *Hoffmann*, 1984].

Fog water with [ALK] < 0 is said to contain inorganic acidity, and its *p*H is lower than that of the reference system. Such fog water has zero buffer capacity with respect to further inputs of strong acids, which may then lead to extremely acidic conditions. We will use the presence of inorganic acidity as an operational definition of the term "acid fog." Alkaline fog water (defined by [ALK] > 0) has a *p*H higher than that of the reference system and will neutralize acid inputs until exhaustion of the alkalinity. However, [ALK] is not a true measure of the acid-neutralizing capacity of the fog water because it ignores exchanges with the gas phase. In particular, alkaline fog water may support a substantial NH_3 vapor pressure [*Jacob et al.*, this issue], which provides an additional source of acid-neutralizing capacity to the fog water. Further, fog water alkalinity depends on the fraction of the aerosol scavenged in the fog. To use alkalinity as a measure of the acid-neutralizing capacity of the atmosphere with respect to acid fog, we need to introduce a more general concept, atmospheric alkalinity.

The atmospheric alkalinity (ALK) (equivalents per cubic meter of air) is the sum of total aerosol alkalinity and gas phase alkalinity in an atmosphere. That atmosphere may or may not contain fog. The reference system is the same as that used for defining fog water alkalinity; gas phase CO_2 and other weak acids are reference species. The aerosol alkalinity $(ALK)_a$ is given by (1), where fog water concentrations (moles per liter of water) are replaced by total aerosol concentrations (moles per cubic meter of air). The gas phase alkalinity is given by the proton donor and acceptor capacities of water-soluble atmospheric gases with respect to the reference system. Atmospheric alkalinity is a conserved quantity upon fog formation and can therefore be used to predict the potential for acid fog from aerosol and gas phase measurements taken under nonfoggy conditions. Atmospheric alkalinity also gives the amount of strong acids that may be emitted to the atmo-

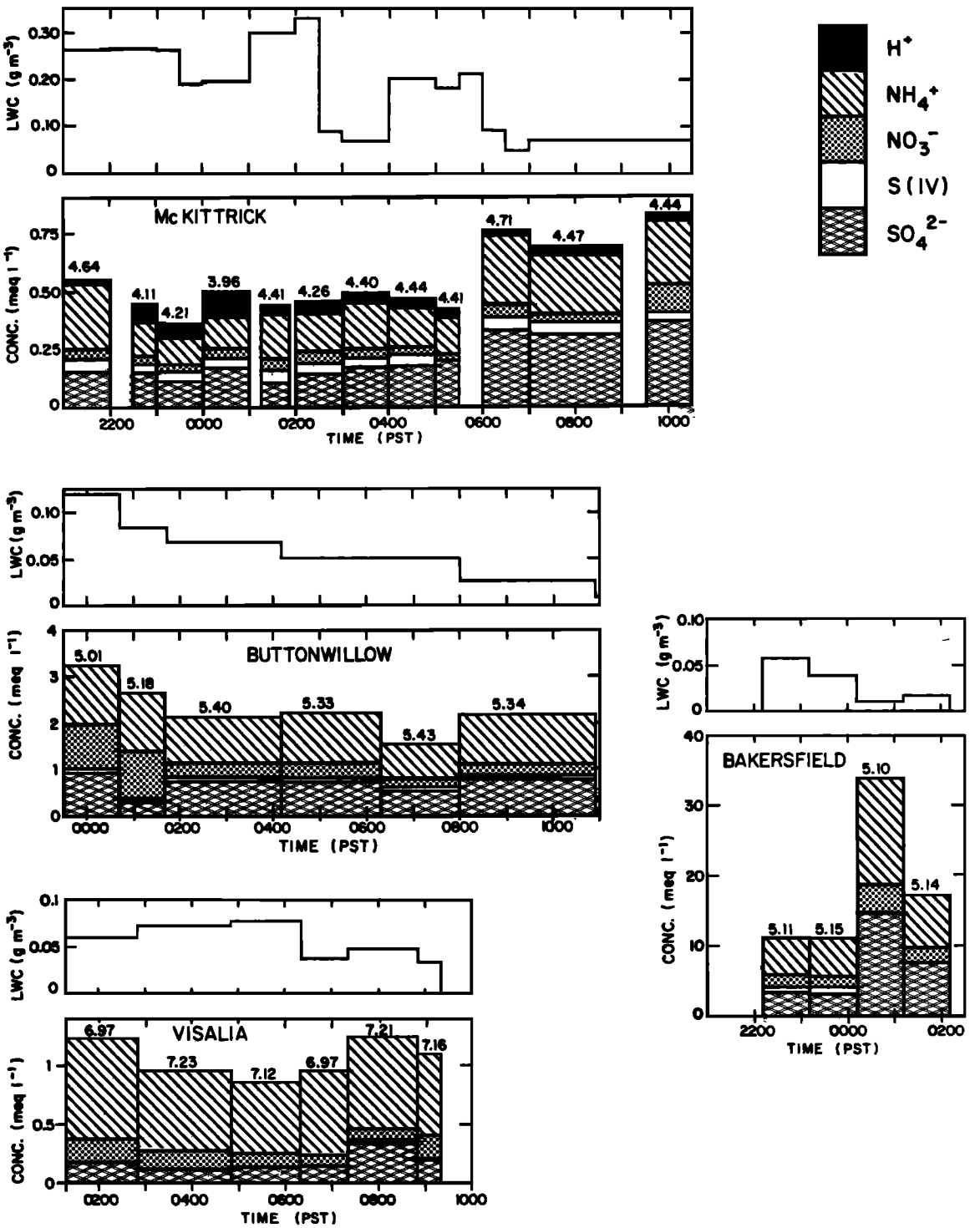

Fig. 4. Fog water composition and liquid water content (LWC) determined simultaneously at four sites during the January 6–7 fog event. The *p*H values are indicated on top of each data bar. Concentrations of S(IV) were not determined in the last two samples at Bakersfield.

sphere before an acid fog problem is to be feared and is thus a useful tool for regulatory purposes.

For the subset of samples analyzed for carboxylic acids we calculated the fog water alkalinity [ALK] as follows:

$$[ALK] = [HCOO^-] + [CH_3COO^-] + [CH_3CH_2COO^-] + [CH_3CH(OH)COO^-] + [HCO_3^-] + [NH_3(aq)] + [OH^-] - [H^+] \quad (2)$$

where $[H^+]$ was directly measured, and the concentrations of alkalinity-contributing species were determined from the fog water concentrations and the equilibrium constants for the acid-base equilibria at 5°C. *Smith and Martell* [1976] and *Martell and Smith* [1977] give K_{a1} values of 1.7×10^{-4} *M*, 1.7×10^{-5} *M*, 1.3×10^{-5} *M*, and 1.3×10^{-4} *M* for HCOOH, CH_3COOH, CH_3CH_2COOH, and $CH_3CH(OH)COOH$, respectively, $K_b = 1.5 \times 10^{-5}$ *M* for NH_3, and $K_w = 2.0 \times 10^{-15}$ M^2 for H_2O dissociation. Concentrations of

TABLE 2. Aerosol, HNO_3(g), and NH_3(g) Data, December 31, 1983 to January 14, 1984

Site	Number of Samples	Na^+	K^+	NH_4^+	Ca^{2+}	Mg^{2+}	Cl^-	NO_3^-	SO_4^{2-}	HNO_3(g)	NH_3(g)	N(V)	N(−III)
Bakersfield	30												
Range		<4–56	<4–19	144–1149	6–75	<4–12	<20–67	85–467	78–855	<4–46	19–483	93–471	209–1204
Mean		15	4	560	35	6	27	276	336	16	146	292	706
Wasco	29												
Range		<4–86	<4–20	74–584	4–43	<4–10	<20–93	23–419	19–312	<4–54	<17–273	54–431	95–648
Mean		12	<4	308	16	<4	22	195	137	19	70	214	378
Lost Hills	25												
Range		<4–48	<4–7	55–553	4–57	<4–11	<20–43	4–310	16–314	<4–174	<17–88	40–414	55–617
Mean		11	<4	223	17	<4	<20	132	108	40	31	172	254
McKittrick	29												
Range		5–70	<4–13	28–424	6–43	<4–10	<20–71	10–246	36–802	<4–164	<17–205	21–347	37–457
Mean		17	<4	224	20	4	21	89	195	34	34	123	258
Buttonwillow[a]	18												
Range		4–51	<4–10	36–663	6–68	<4–11	<20–41	34–400	31–579	<4–37	18–645	77–406	135–1001
Mean		19	<4	306	31	5	23	184	188	12	131	196	437
Visalia[b]	14												
Range		<4–16	<4–7	108–359	6–37	2–5	<20–41	73–318	35–129	<4–15	184–662	73–322	484–869
Mean		7	<4	239	20	<4	<20	175	83	7	450	182	689
Lake Isabella	11												
Range		<4–28	<4–4	<8–32	6–32	<4	<20	<4–23	<4–23	5–36	<17–44	<8–59	<8–44
Mean		10	<4	8	11	<4	<20	9	9	16	19	25	27
Tehachapi	13												
Range		<4–93	<4–140	<8–73	10–126	<4–43	<20–252	<4–50	<4–47	<4–18	<17–74	<8–68	<8–84
Mean		17	12	11	46	8	32	11	17	7	34	18	45

Values are in nanoequivalents per cubic meter. See *Jacob* [1985] for the complete data set.
[a]From January 5 to January 14.
[b]From December 31 to January 7.

HCO_3^- were calculated by assuming equilibrium with $P_{CO2} = 340$ ppm ($H \times K_{a1} = 7.07 \times 10^{-6}\ M^2\ atm^{-1}$ at 5°C). We assumed $[S(IV)^{2-}] = 0$ in all our calculations; free S(IV) is mostly divalent at $pH > 7$, but there is strong evidence that S(IV) in fog water actually combined with aldehydes to form stable adducts [*Munger et al.*, 1984]. These S(IV)-aldehyde adducts remain monovalent over a higher range of pH, up to pH 11.7 for the S(IV)-formaldehyde adduct [*Sørensen and Andersen*, 1970]. Even if S(IV) was actually divalent at $pH > 7$, S(IV) concentrations in fog water at such high pH values were low (Table 3, Visalia), and the contribution of $S(IV)^{2-}$ to the fog water alkalinity would be very small.

Estimating $(ALK)_a$ from the available aerosol data was less straightforward. We assumed that the ions on the right-hand side of (1), possibly plus additional weak acid anions, constituted the aerosol ionic content unaccounted for in our chemical analysis. By a charge balance on the aerosol we obtained:

$$(ALK)_a = (Na^+) + (K^+) + (NH_4^+) + 2(Ca^{2+}) + 2(Mg^{2+}) - (Cl^-) - (NO_3^-) - 2(SO_4^{2-}) \quad (3)$$

Since we have argued that the inorganic acidity in fog is mostly controlled by species in the H_2SO_4-HNO_3-NH_3 system, we will assume that the only gas phase contributors to (ALK) are HNO_3(g) and NH_3(g). A calculation of the ultimate alkalinity of an air parcel should include SO_2(g); however, the contribution of SO_2(g) to (ALK) may be limited by the slow rate of SO_2 scavenging by fog [*Jacob and Hoffmann*, 1983]. For now we ignored the SO_2(g) contribution and calculated the atmospheric alkalinity from the expression:

$$(ALK) = (ALK)_a + (NH_3(g)) - (HNO_3(g)) \quad (4)$$

Average alkalinities at each site are given in Table 4*a*. Because of the possibility of HNO_3 or NH_3 volatilization from aerosol filter samples collected in fog (see appendix), (ALK) and $(ALK)_a$ were calculated only for nonfoggy conditions. (ALK) and $(ALK)_a$ were usually small numbers determined by the difference of two large numbers, so the standard errors were fairly large. The calculation of the fog water alkalinity [ALK] involved subtracting a small number from a large number; the resulting standard errors were small and were not indicated explicitly.

TABLE 3*a*. Liquid Water-Weighted Average For Water Concentrations of Major Ions, December 31, 1983, to January 14, 1984

Site	Number of Samples	pH Range	H^+	Na^+	NH_4^+	Ca^{2+}	Mg^{2+}	Cl^-	NO_3^-	SO_4^{2-}	S(IV), μM	L^a, g m^{-3}
Bakersfield	16	5.10–6.92	2.0	42	3270	169	33	122	819	2070	384	0.057
McKittrick	58	2.68–5.23	93	11	480	39	5	15	250	345	43	0.11
Buttonwillow	7	5.01–6.79	5.6	13	1067	82	10	47	522	760	74	0.050
Visalia	13	5.51–7.23	0.1	6	1080	17	2	115	341	265	12	0.049

Unless otherwise indicated, concentrations are in microequivalents per liter of water. See *Jacob* [1985] for the complete data set.
[a]Average liquid water content, based on the total amount of water collected and the total sampling time.

TABLE 3b. Liquid Water-Weighted Average Fog Water Concentrations of Trace Metals, December 31, 1983, to January 14, 1984

Site	Number of Samples	Fe	Mn	Pb	Cu	Ni	V
Bakersfield	5	438	31	134	19	29	41
McKittrick	42	76	6	27	12	48	91
Buttonwillow	6	142	17	44	82	44	32
Visalia	6	144	7	61	7	11	8

Concentrations are in micrograms per liter of water. See *Jacob* [1985] for the complete data set.

The western edge of the SSJV currently suffers from a general acid fog problem, as shown by the negative average values of (ALK). In the remainder of the valley, (ALK) > 0, and fog water is not usually acidic. However, the average values of (ALK) at Bakersfield and Wasco presently amount to less than 20% of (S(VI) + N(V)) equivalent concentrations. If NH_3 emissions in the SSJV decrease by 20% compared to their current level, for example, because of a decline of the cattle industry or fluctuations in the soil moisture and temperature, a general acid fog situation in the east side of the SSJV will result. The same result will be achieved by a 20% increase in (S(VI) + N(V)) equivalent concentrations due to a rise in SO_2 and NO_x emissions. Fog water alkalinity at Visalia will not be affected by these changes in SSJV emissions, considering the large (ALK)/(S(VI) + N(V)) ratio at that site; therefore there is little risk that an acid fog problem in the SSJV could spread to the northern part of the San Joaquin Valley.

The partitioning of the atmospheric alkalinity between the gas phase and the aerosol is of interest. Scavenging of NH_3(g) to form ammonium salts of weak acids could be a source of important alkalinity in the aerosol or fog water. Indeed, significant alkalinities were found in fog water; however, aerosol collected under nonfoggy conditions was never significantly alkaline. Although the error bars on the determinations of $(ALK)_a$ were large, the absence of positive $(ALK)_a$ values in the presence of large excesses of NH_3(g), as at Visalia, strongly suggests that the alkaline ammonium salts are volatile under nonfoggy conditions. This hypothesis is supported by concurrent sampling of aerosol and fog water at Visalia, where NH_4^+ was in excess of NO_3^- and SO_4^{2-} in the fog water but not in the dried aerosol. Artifact aerosol neutralization should not occur during filter storage (see appendix).

Under nonfoggy acidic conditions the aerosol contained significant inorganic acidity when S(VI) was present in excess of N(−III). This occurred in six of the samples, all at McKittrick. In the remainder of the samples collected under acidic conditions the aerosol was neutralized, and the inorganic acidity was entirely present in the gas phase as HNO_3(g). This observation is in agreement with aerosol equilibrium models [*Bassett and Seinfeld*, 1983]; NH_3(g) is scavenged by acid sulfate aerosol until this aerosol is neutralized as $(NH_4)_2SO_4$. Excess NH_3 may then combine with HNO_3 to add NH_4NO_3 to the aerosol phase, but HNO_3 in excess of NH_3 remains in the gas phase.

TABLE 3c. Liquid Water-Weighted Average Fog Water Concentrations of Carboxylic Acids, December 31, 1983, to January 14, 1984

Site	Number of Samples	Formate	Acetate	Lactate	Propionate
Bakersfield	2	45	155	15	9
McKittrick	26	22	3	2	0
Buttonwillow	2	144	59	3	0
Visalia	6	53	65	7	0

Concentrations are in micromols per liter of water. See *Jacob* [1985] for the complete data set.

TABLE 4a. Average Alkalinities at Each Site

Site	Number of Samples	ALK, neq m^{-3}	ALK_a, neq m^{-3}	ALK_f, μeq L^{-1}	L,[a] g m^{-3}
Bakersfield	28	111 ± 31	−20 ± 30		
Wasco	27	46 ± 19	−13 ± 18		
Lost Hills	23	−11 ± 16	−2 ± 16		
McKittrick	21	−12 ± 18	−20 ± 17		
Buttonwillow[b]	17	131 ± 31	−14 ± 28		
Visalia[c]	11	441 ± 30	−7 ± 18		
Bakersfield	2			210	0.11
McKittrick				−98	0.11
Buttonwillow[b]				183	0.05
Visalia[c]				220	0.03

ALK is the atmospheric alkalinity, ALK_a is the aerosol alkalinity, ALK_f is the fog water alkalinity. ALK and ALK_a were calculated only for nonfoggy periods. ALK_f was calculated for the subset of samples analyzed for organic acids. Error bounds are the standard errors on the determinations of the means.

[a]Average liquid water content for the subset of fog water samples.
[b]From January 5 to January 14.
[c]From December 31 to January 7.

The contributions of different species to fog water alkalinity are shown in Table 4b. The main contributors to [ALK] at Bakersfield and Buttonwillow were formate and acetate. Formic and acetic acids are efficiently scavenged in fog water at pH > 5; they are highly soluble, as indicated by their large Henry's law constants ($H_{HCOOH,298} = 3.7 \times 10^3$ M atm^{-1}, $H_{CH3COOH,298} = 8.8 \times 10^3$ M atm^{-1} [*Weast*, 1984]), and they are mostly dissociated, as indicated by their acidity constants (see above). At Visalia the fog water pH was much higher than at Bakersfield or Buttonwillow, and the contribution from HCO_3^- to [ALK] was correspondingly larger. Carboxylate anions did not provide higher contributions at Visalia than at Bakersfield or Buttonwillow; since carboxylic acids are already efficiently scavenged at pH 5–6, raising the pH higher leads to little additional scavenging.

ACCUMULATION AND REMOVAL OF H_2SO_4-HNO_3-NH_3 SPECIES OVER THE COURSE OF A SEVERE STAGNATION EPISODE

The goal of this section is to interpret the accumulation of S(VI), N(V), and N(−III) species over the course of the January 2–7 severe stagnation episode, in terms of atmospheric production and removal mechanisms. As shown in Figure 5, the stagnation episode was generally associated with high concentrations of S(VI), N(V), and N(−III). The inversion base was roughly stable at h = 400 m AGL throughout the episode, and the residence time for air parcels in the SSJV was $\tau_a = 5$ days. Therefore deposition was a more important removal pathway than ventilation for species with deposition velocities >0.1 cm s^{-1}. The highest concentrations on the SSJV floor (Bakersfield, Wasco, and Lost Hills) were observed on January 5, after 4 days of stagnation under nonfoggy, overcast conditions; low aerosol deposition rates in the absence of fog allowed high levels of pollutant accumulation. Dense, widespread valley fogs on the mornings of January 6 and 7 (Figure 2) were associated with general decreases in aerosol con-

TABLE 4*b*. Contributions of Different Species to Fog Water Alkalinity

Site	Number of Samples	Free Acidity,[a] μeq L^{-1}	Formate, μeq L^{-1}	Acetate, μeq L^{-1}	Lactate, μeq L^{-1}	Propionate, μeq L^{-1}	HCO_3^-, μeq L^{-1}	NH_3(aq), μeq L^{-1}
Bakersfield	2	−1	45	134	15	9	6	<1
McKittrick	38	−123	22	1	2	<1	<1	<1
Buttonwillow	2	−8	142	44	3	<1	1	<1
Visalia	6	<1	53	65	7	<1	92	2

Contributions calculated from fog water *p*H.
[a]Free acidity = $[H^+] - [OH]$.

centrations, probably due to rapid deposition of fog droplets. *Jacob et al.* [1984*a*] have previously suggested that enhanced aerosol deposition in fogs efficiently limits pollutant accumulation during stagnation episodes, and our data support this hypothesis. Further decreases in atmospheric concentrations were observed on January 7–8, due to the rise of the inversion base (Figure 2) and deposition from drizzle.

As S(VI) and N(V) were produced over the course of the stagnation episode, significant inorganic acidities were observed at Wasco, Lost Hills, and McKittrick. At Bakersfield, sufficient N(−III) was available to totally neutralize acid inputs. Because of the remarkably stable mixing height and the lack of ventilation we can attempt to apply stirred-tank considerations to calculate the rates of H_2SO_4 and HNO_3 production in the SSJV. The residence time τ of a species in a stirred tank is given by the expression:

$$\frac{1}{\tau} = \frac{v}{h} + \frac{1}{\tau_a} + k \qquad (5)$$

where v is the deposition velocity and k is a first-order chemical loss rate. Of special interest is the period January 2–5, ranging from the onset of stagnation to the first widespread valley fog. The SSJV floor (Bakersfield, Wasco, and Lost Hills) remained overcast throughout that period, and roughly constant values of v and k may be expected. We can thus follow the evolution over 4 days of a very well-controlled stagnant atmospheric system.

Production of H_2SO_4

Concentrations of S(VI) increased progressively on the SSJV floor during the nonfoggy January 2–5 period. Concentrations remained very low at Visalia, which is out of the SSJV and far from SO_2 sources. Sulfur dioxide, the main precursor of S(VI) in the SSJV, has a deposition velocity of the order of 1 cm s^{-1} over grass [*Sehmel*, 1980]. A steady state for SO_2 in the SSJV should therefore be approached on a time scale of the order of 1 day after the onset of stagnation, and this appeared to be the case at Kernridge (Figure 2). Measured concentrations of SO_2 at Bakersfield, Kernridge, and Lost Hills during January 3–5 averaged 25, 12, and 3 ppb, respectively; a strong spatial gradient in SO_2 concentrations was maintained because mixing was slow. Modeling of SO_2 transport under stagnant conditions [*Aerovironment, Incorporated*, 1984] indicates that the SO_2 concentration field in the SSJV should be bounded on the lower end at Wasco and Lost Hills and on the upper end at Bakersfield. Therefore we expect steady state SO_2 concentrations in the SSJV mixed layer to range between 3 and 25 ppb. A stirred-tank calculation based on the volume of the SSJV mixed layer and the emission data of Table 1, assuming chemical loss to be slower than deposition ($V_{SO_2} = 1$ cm s^{-1}), gives an average steady state SO_2 concentration of the order of 9 ppb in the SSJV. This is consistent with our observations.

The accumulation pattern of S(VI) on the SSJV floor was consistent with a pseudo first-order conversion rate of SO_2 to S(VI). Concentrations of S(VI) increased relatively steadily during the January 3–5 period, when SO_2 concentrations were approaching steady state. This steady conversion of SO_2 maintained important differences in S(VI) concentrations from site to site within the SSJV. A time lag for S(VI) production was clearly seen at Bakersfield on January 2, attributable to the time required for SO_2 to accumulate after the onset of stagnation. The profiles of S(VI) concentrations in the SSJV did not suggest an approach of steady state by January 5; the residence time of S(VI) aerosol in the SSJV under nonfoggy conditions was thus longer than 3 days, indicating a deposition velocity $v_{S(VI)} < 0.05$ cm s^{-1} (equation (5)). This is in agreement with predicted deposition velocities for particles in the 0.05- to 1-μm size range at low wind velocities [*Sehmel*, 1980]. Over the period January 3–5, S(VI) was produced in the SSJV much faster than it was removed, and we can to a first approximation equate the observed rate of S(VI) accumulation to the rate of SO_2 conversion. The average rates of S(VI) accumulation during January 3–5 were 9 neq m^{-3} h^{-1} at Bakersfield, 3 neq m^{-3} h^{-1} at Wasco, and 3 neq m^{-3} h^{-1} at Lost Hills; from the assumed steady state SO_2 concentration field in the SSJV (range 3–25 ppb, average 9 ppb), we estimate an average SO_2 conversion rate in the range 0.4–1.1% h^{-1}.

Because of the lack of photochemical activity during the stagnation episode (see Figure 6 and discussion below), conversion of SO_2 to H_2SO_4 must have proceeded predominantly in the aerosol and the cloud droplets. A likely pathway is metal-catalyzed autoxidation in the aqueous phase [*Hoffmann and Jacob*, 1984], which does not require photochemically generated oxidants. Considering that a stratus cloud filled a large fraction of the mixed layer during the period of January 3–5, an important question is to determine if the principal site for S(IV) oxidation was the cloud or the haze aerosol below. Concentrations of SO_2 progressively decreased at Kernridge during the foggy January 5–7 period, while concentrations of CO and NO*x* (which was emitted from the same sources as SO_2) kept on increasing. This is strong evidence that removal of SO_2 from the atmosphere was enhanced in the presence of fog. From Figure 2 the rate of SO_2 scavenging by fog appears to be on the order of 5% h^{-1}. This enhanced scavenging of SO_2 in fog does not necessarily imply enhanced production of S(VI); S(IV) may be stabilized in the aqueous phase by formation of adducts [*Munger et al.*, 1983, 1984] or removed by deposition before being oxidized. We tried to evaluate S(VI) production directly in fog droplets by comparing S(VI) concentrations in successive fog water samples collected at one site, using Ni and V as conservative tracers for sulfur. However, we did not obtain statistically significant rates of SO_2 conversion in fog water ($2 \pm 6\%$ h^{-1} at Bakersfield, $0 \pm 3\%$ h^{-1} at McKittrick [see *Jacob*, 1985]). This failure to find statistically significant rates is probably due to the complex nature of fog droplet growth and transport.

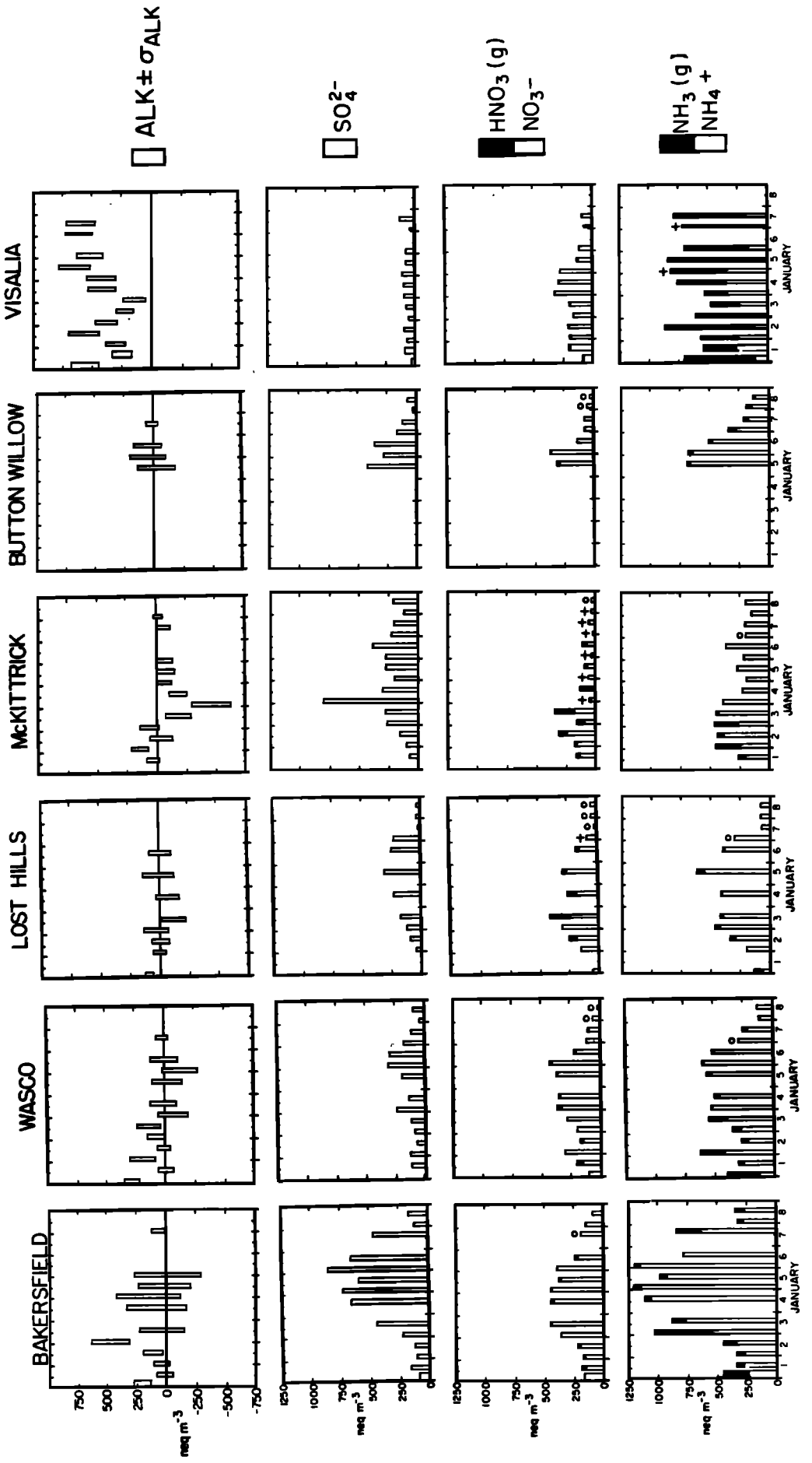

Fig. 5. Aerosol and gas phase concentrations and atmospheric alkalinities at the six valley sites over the period January 1–8. An open circle on top of the data bar indicates that the gas phase species was not measured. A plus sign on top of the data bar indicates that volatilization from the filter in fog could have affected the aerosol measurement (see the appendix).

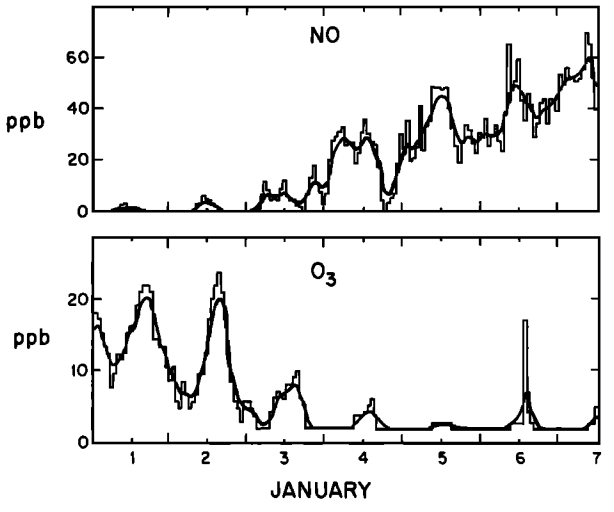

Fig. 6. Concentrations of NO and O_3 at Kernridge. The bold lines were obtained by smoothing the data with a digital filter.

Production of HNO_3

In addition to H_2SO_4, HNO_3 was produced. However, N(V) did not accumulate as steadily as S(VI). Concentrations of N(V) in the SSJV increased rapidly at the onset of stagnation (January 2–3) but did not increase after January 3. Nitrogen oxides accumulated steadily throughout the stagnation episode (Figure 2), showing no indication of loss from chemical conversion. Concentrations of N(V) did not show the large differences from site to site that were observed for S(VI), even though SO_2 and NO_x mostly originated from the same combustion sources.

A logical explanation for these observations is that the rate of HNO_3 production was slow during the stagnation episode because of the widespread and persistent low overcast. Figure 6 shows the NO and O_3 concentration profiles at Kernridge. Ozone levels prior to the onset of stagnation were relatively high, indicating substantial photochemical activity; HNO_3 production by the reaction $NO_2 + OH$ should proceed rapidly under those conditions. Also, O_3 was always present in excess of NO, so that HNO_3 could be produced at night by heterogeneous pathways initiated by the reaction $NO_2 + O_3$ [*Heikes and Thompson*, 1983]. After the onset of stagnation, however, the overcast restricted photochemical activity, and very low O_3 concentrations were observed; OH concentrations were probably very low. Further, since NO progressively accumulated to levels sufficient to titrate O_3 fully, the reaction $NO_2 + O_3$ did not proceed. Therefore little secondary production of HNO_3 would be expected in the SSJV after January 3. Fog did not perceptibly enhance the conversion of NO_x to HNO_3; concentrations of NO_x at Kernridge kept on increasing during the January 5–7 foggy period, similarly to CO, which is not water-soluble. This is consistent with the poor solubilities of NO and NO_2 in water at atmospheric concentrations [*Schwartz and White*, 1981].

The NO_3^- aerosol present after January 3 was therefore mostly aged aerosol, slowly mixing within the SSJV. As mixing proceeded, the differences in NO_3^- concentrations from site to site became progressively weaker. Concentrations of N(V) at Bakersfield and Wasco were similar on January 4–5, even though S(VI) concentrations were much higher at Bakersfield. At Lost Hills and McKittrick, acidification of the atmosphere coincided with a brief increase in HNO_3(g) concentrations, immediately followed by an important drop in total N(V) concentrations. This indicates displacement of NO_3^- by H_2SO_4 in the aerosol, followed by rapid deposition of HNO_3(g). The atmospheric lifetime for HNO_3(g) is thus short (<0.5 days), which implies a large deposition velocity (>1 cm s^{-1}).

Accumulation of NH_3

Almost all of the NH_3 emitted in the SSJV during the stagnation episode was used to neutralize acid inputs. The fate of the resulting (SO_4^{2-}, NO_3^-, NH_4^+) aerosol has been discussed above. At Visalia, however, acid inputs were small, and a large fraction of total N(−III) remained in the gas phase as NH_3(g). No accumulation of NH_3(g) was apparent at that site over the course of the episode, and this suggests an atmospheric residence time of <0.5 days for NH_3(g) (deposition velocity of >1 cm s^{-1}). Frequent fog and drizzle after January 5 at Visalia resulted in an important depletion of NH_4^+ aerosol, but NH_3(g) concentrations were unaffected. Ammonia is poorly scavenged at the high *p*H values typical of Visalia fog water [*Jacob et al.*, this issue].

Stirred-Tank Simulation

The above discussions have shown that the profiles of concentrations versus time during a stagnation episode can be successfully interpreted, based on stirred-tank considerations of pollutant accumulation and removal; however, the differences in concentrations from site to site clearly indicate that a stirred-tank model for the SSJV as a whole is not an adequate modeling tool. The major reason is that internal mixing is slow. Nevertheless, the success of the stirred-tank model in interpreting the data at individual sites suggests that one could model the SSJV by subdividing it into a number of cells where the stirred-tank approximation could be properly invoked. Such an exercise is beyond the scope of this paper; however, for the sake of illustrating and summarizing our discussion of field data we will present the results of a stirred-tank calculation applied to the entire SSJV. The accumulation of constituent A in such a model is described by

$$d(A)/dt = E_A + k'(B) - k(A) - \frac{1}{h}[(A_g)v_{A_g} + (A_a)v_{A_a} + (A_f)v_{A_f}] - (A)/\tau_a \quad (6)$$

where A_g, A_a, and A_f are the gas phase, aerosol phase, and fog water phase species, respectively, E_A is the emission rate averaged over the volume of the mixed layer (moles per cubic meter per day), and k' is the pseudo first-order rate for conversion of precursor B to A. We simultaneously solved the coupled stirred-tank equations for SO_2, NO_x, S(VI), N(V), and N(−III). The model conditions are given in Table 5 and are for the most part deduced from our discussion of the field data. The emission data are those of Table 1, averaged over the volume of the SSJV mixed layer. We assumed that the aerosol was a neutralized mixture under nonfoggy conditions if N(−III) was in excess of S(VI), and that the formation of NH_4NO_3 aerosol was sufficiently favored to prevent HNO_3 and NH_3 from coexisting in the gas phase under any condition (valid if the atmosphere is sufficiently humid). The simulation was run for 4 days from the beginning of the episode, with a foggy period extending from $t = 2$ days to $t = 3$ days. On the basis of results presented by *Jacob* [1985], *Jacob et al.* [this issue], and *Waldman* [1986] we made the simplifying assumptions that (1) 30% of the aerosol is present in the fog water at any given time, (2) HNO_3(g) is 100% scavenged under all foggy conditions, and (3) NH_3(g) is 100% scavenged

in fog under acid conditions but not scavenged at all under alkaline conditions.

Figure 7 shows the predicted concentration profiles. Aerosol accumulates rapidly under nonfoggy conditions and is partially removed by fog. The main features of the observed concentration profiles are reproduced, in particular, the accumulation patterns for SO_4^{2-} and NO_3^-. The emission rates of Table 1 lead to concentrations of species that are in the range of those observed. Some excess alkalinity as NH_3(g) remains present throughout the episode.

CONCLUSION

A systematic characterization of the H_2SO_4-HNO_3-NH_3 system in the fog water, the aerosol, and the gas phase was conducted at a network of sites in the San Joaquin Valley of California. Spatial patterns of atmospheric concentrations reflected the geographic distribution of oil recovery operations (SO_2, NO_x) and livestock-feeding and agricultural activities (NH_3). The acidity of the fog water was found to be determined by the relative abundances of local acidic (SO_2, NO_x) and alkaline (NH_3) emissions. A region of prevailing acidic conditions was identified on the western edge of the valley, where NH_3 emissions were low. Elsewhere, sufficient NH_3 was available to fully titrate the acidity. In the southern end of the valley, where major oil recovery operations release large amounts of SO_2 and NO_x, a precarious atmospheric balance was found between high concentrations of acids and bases.

The concept of atmospheric alkalinity was introduced as a quantitative measure of the acid-neutralizing capacity of the atmosphere with respect to fog. On the basis of this concept we predicted the regional potentials for high-acidity fog events in the San Joaquin Valley. We concluded that small changes in the activities of the agricultural industry or the oil industry could lead to widespread "acid fog" in the southern end of the valley.

Pollutant concentrations in the valley were strongly affected by the height of the mixed layer and by the occurrence of drizzle or fog. Mixing heights above 1000 m AGL efficiently ventilated the valley. A severe stagnation episode was documented when a temperature inversion based a few hundred meters above the valley floor persisted for 6 days. Progressive accumulation of H_2SO_4-HNO_3-NH_3 species in the mixed layer was observed and interpreted in terms of atmospheric production and removal mechanisms. The accumulation patterns were consistent with very low deposition velocities for secondary (SO_4^{2-}, NO_3^-, NH_4^+) aerosol under nonfoggy conditions (<0.05 cm s^{-1}), and high deposition velocities for HNO_3(g) and NH_3(g) (>1 cm s^{-1}). Decreases in aerosol concentrations were observed following fogs and were attributed to the rapid deposition of fog droplets. Therefore the occurrence of fog was found to effectively limit pollutant accumulation during stagnation episodes.

Secondary production of strong acids under stagnant conditions entirely titrated available alkalinities at the sites farthest from NH_3 emissions. A steady conversion rate of SO_2 to H_2SO_4 was estimated at 0.4–1.1% h^{-1} under overcast stagnant conditions. Conversion of NO_x to HNO_3 was rapid at the beginning of the episode but dropped as the widespread and persistent low overcast reduced photochemical activity. Removal of SO_2 was found to be enhanced in fog, compared to nonfoggy conditions, but NO_x was not scavenged in fog. Acidification of the atmosphere was associated with a brief increase in HNO_3(g) followed by a drop in total N(V) concentrations; this was explained by the displacement of aerosol NO_3^- by H_2SO_4, followed by rapid deposition of HNO_3(g).

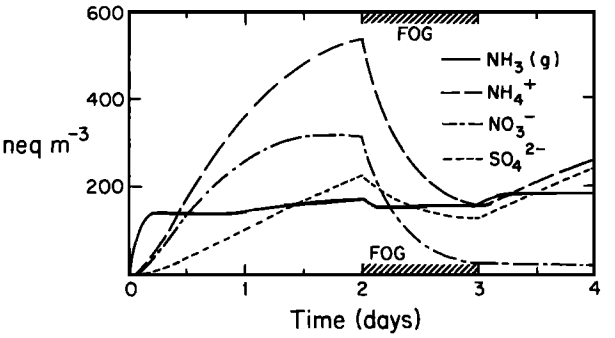

Fig. 7. Stirred-tank simulation of pollutant accumulation in the SSJV over the course of a stagnation episode. The simulation conditions are given in Table 5.

TABLE 5. Parameters for Stirred-Tank Model Simulation

	Deposition velocities, cm s^{-1}
SO_2	1
NO_x	0.1
Nonactivated aerosol	0.05
fog droplets	4
HNO_3(g)	3
NH_3(g)	3
	Conversion rates, % h^{-1}
$SO_2 \rightarrow SO_4^{2-}$, no fog	1
$SO_2 \rightarrow SO_4^{2-}$, fog	5
$NO_x \rightarrow NO_3^-$	10 exp ($-2t$)
	Emission rates, μmol m^{-3} d^{-1}
SO_2	0.95
NO_x	1.3
NH_3	1.4

Residence time of air parcels: 5 days. Mixing height: 400 m AGL; Initial conditions: (H_2SO_4) = (HNO_3) = (NH_3) = 0 at $t = 0$; Fog from $t = 2$ to $t = 3$, t is stated in days throughout.

APPENDIX: ERROR ANALYSIS

Fog Water Concentrations

A recent intercomparison study of fog water collectors [*Hering and Blumenthal*, 1985; *Waldman*, 1986] has demonstrated that the California Institute of Technology rotating arm collector provides reproducible and representative samples under both light and heavy fog conditions. The uncertainty on the concentrations of major ions (determined from samples collected with two rotating arm collectors set side by side) was found to be about 15%. Errors due to chemical analysis in the laboratory were about 5% for all analyzed ions. No significant differences in ionic concentrations were found between samples collected concurrently with the rotating arm collector, a jet impactor [*Katz*, 1980], and a screen collector [*Brewer et al.*, 1983], set side by side.

Ionic balances are an indicator of whether all ionic components in the sample have been accounted for in analysis. Ionic

balances in the fog water samples were 0.98 ± 0.18 at Bakersfield ($n = 15$), 1.02 ± 0.09 at McKittrick ($n = 53$), 1.11 ± 0.18 at Buttonwillow ($n = 7$), and 0.60 ± 0.17 at Visalia ($n = 12$). The ionic balances were calculated from the following molar ratio:

$$\text{Ionic balance} = \frac{[Cl^-] + [NO_3^-] + 2[SO_4^{2-}] + [\text{S IV}]}{[H^+] + [Na^+] + [NH_4^+] + 2[Ca^{2+}] + 2[Mg^{2+}]} \quad \text{(A1)}$$

where S(IV) was assumed to be monovalent [*Jacob and Hoffmann*, 1983]. We have argued previously (equation (2)) that this is a good assumption even at high *p*H. The most reliable ionic balances were found at McKittrick, while at Visalia there was a considerable and consistent anion deficiency. Fog water at Visalia had a consistently high *p*H and as a consequence could contain important alkalinity; therefore additional weak acid anions must be considered in an ionic balance. In fog water with low *p*H, such as at McKittrick, weak acids are mostly present in undissociated form and thus (A1) represents a good balance of cations to anions.

The principal ionic contributors to alkalinity in the *p*H range 3–8 are expected to be HCO_3^- and carboxylate ions. Fog water concentrations of four carboxylate ions were determined on a subset of the fog water data set (Table 3). For that subset we calculated the concentrations of the anionic forms of the weak acids from equilibrium at the fog water *p*H and with the acidity constants given in the text. Before inclusion of weak acids the ionic balances were 1.03 ± 0.09 at McKittrick ($n = 25$) and 0.49 ± 0.15 at Visalia ($n = 6$); after inclusion of weak acids the ionic balances were 1.06 ± 0.11 at McKittrick and 0.75 ± 0.15 at Visalia. The McKitrick samples had little alkalinity, and the ionic balance remained close to unity. At Visalia on the other hand, ionic balances were greatly improved. There was still an anion deficiency at Visalia, likely due to undetermined weak acids.

Aerosol, HNO_3(g), and NH_3(g) Concentrations

The filter methods used in this study may lead to two major types of error: (1) N(V) and N(−III) artifacts, and (2) random errors from the sampling process. We will address each in order. An additional source of error could be the neutralization of acidic and alkaline aerosol by absorption of NH_3(g) and HNO_3(g), respectively, during filter storage; however, blank oxalic-acid-impregnated filters and nylon filters were found to remain blank even after extended storage. Therefore aerosol neutralization during storage did not seem to occur.

Stelson and Seinfeld [1982] have shown that an increase in temperature at constant dew point during sampling may volatilize ammonium nitrate collected on Teflon filters and result in artifact HNO_3(g) and NH_3(g). Further, absorption of gaseous nitric acid on the Teflon filter may result in artifact aerosol nitrate [*Spicer and Schumacher*, 1979; *Appel et al.*, 1980]. In an intercomparison study of gaseous nitric acid measurement methods, *Spicer et al.* [1982] found good agreement between the dual-filter method (used here) and other methods. Further, they found that the dual-filter method was accurate in measuring total N(V).

The study of *Spicer et al.* [1982] was conducted under hot, dry conditions. Potential biases are different under the cool, humid conditions found in the San Joaquin Valley. Nighttime samples (0000–0400 PST) were probably unaffected by volatilization because temperatures during the sampling period either remained constant or decreased. During the day, temperature changes were usually small because of the overcast conditions; temperatures recorded hourly at Bakersfield between 1200 and 1600 PST increased on only five of the 15 sampling days and never increased by more than 1°C, except on January 14 (when a 3°C increase was observed). Still, an increase of 1°C in temperature at constant dew point may increase the dissociation constant $K = P_{HNO_3} \times P_{NH_3}$ by a factor of 2 under high-humidity conditions [*Stelson and Seinfeld*, 1982]. The formation of aerosol ammonium nitrate is strongly favored thermodynamically, and aerosol concentrations could not be significantly affected by volatilization; on the other hand, high relative errors may occur in the determination of the gas present at the lowest concentration. Since that concentration was often near or below the detection limit, the error was of little consequence.

Teflon filters run in dense fogs accumulated drops of liquid water at the surface. In those particular cases the filters were dried in the open before being sealed. Nitric acid scavenged in acidic fog volatilizes during drying, leading to an underestimate of total aerosol NO_3^-. No significant NO_3^- loss should occur in nonacidic fog because in that case NO_3^- remains in the aerosol phase as the fog dissipates. Similarly, NH_4^+ aerosol should not volatilize in acidic fog. Volatilization of NH_4^+ from filters collected in alkaline fog depends on the stability of the ammonium salts of weak acids, which appear to be volatile; some volatilization of NH_4^+ was found to occur in a sample collected during fog at Visalia [*Jacob*, 1985].

"Random errors" are of three types: (1) uncertainty in the flow rate through the filter, (2) uncertainty in the efficiency of recovery by extraction, and (3) analytical error. Because the first two sources of error affect the sample as a whole, we expect a correlation to exist between the errors on the different species. To test for these errors, concentrations of SO_4^{2-}, NO_3^-, and NH_4^+ were determined in duplicate for $n = 45$ pairs of filter samples "1" and "2," collected side by side. Concentrations of Cl^- were also determined, but the errors on those concentrations were generally lower than the Cl^- filter blank. The relative differences in the determinations of X for the 45 pairs of duplicate samples were statistically analyzed as follows:

$$D_X = \frac{2(X_2 - X_1)}{X_1 + X_2} \quad \text{(A2)}$$

$$\sigma = \left[\frac{\sum (D_X)^2}{n}\right]^{1/2} \quad \text{(A3)}$$

Standard deviations σ on the determination of SO_4^{2-}, NO_3^-, and NH_4^+ were 18.6, 18.8, and 19.1%, respectively. These results are comparable to those reported by *Russell and Cass* [1984] for similar measurements. Student "*t*" tests for paired data at the 5% level of significance did not show significant differences between sampling positions 1 and 2 for SO_4^{2-}, NO_3^-, or NH_4^+ at any site, therefore no significant effects from the differences in backup filters were apparent.

We found $D_{SO_4^{2-}}$, $D_{NO_3^-}$, and $D_{NH_4^+}$ to be strongly correlated ($r^2 = 0.71$ between $D_{SO_4^{2-}}$ and $D_{NH_4^+}$, $r^2 = 0.69$ between $D_{NO_3^-}$ and $D_{NH_4^+}$). These correlations must be taken into account in the error analyses of quantities calculated by differences of concentrations, such as (ALK) or gas phase concentrations predicted by thermodynamic models [*Jacob et al.*, this issue]. We resolved σ into its component σ_P, associated with pump operation and filter extraction, and its component $\sigma_{A,X}$, associated with chemical analysis. The error char-

acterized by σ_P may be assumed to be the same for SO_4^{2-}, NO_3^-, and NH_4^+, while the errors due to analysis should be uncorrelated. Because σ is small, we can write as an approximation:

$$\sigma^2 = \sigma_P^2 + \sigma_{A,X}^2 \quad \text{(A4)}$$

By statistical analysis of the differences between NH_4^+, NO_3^-, and SO_4^{2-} concentrations we obtained $\sigma_P = 18.1\%$, $\sigma_{A,SO_4^{2-}} = 4.4\%$, $\sigma_{A,NO_3^-} = 5.1\%$, and $\sigma_{A,NH_4^+} = 6.3\%$. These analytical errors are consistent with our laboratory precision.

No duplicate analyses were made for Na^+, K^+, Ca^{2+}, and Mg^{2+}. Replicate analyses of standards indicate $\sigma_{A,X}^2$ of about 5% for these four ions. Duplicates for NH_3(g) and HNO_3(g) determinations were not collected, but the $\sigma_{A,X}^2$ values should be the same as for NH_4^+ and NO_3^-, respectively. In addition to the analytical error, concentrations of all constituents were assumed to be subject to the same error σ_P. This assumption implies that the variability of the flow rate through the filter is the major contributor to σ_P, which seems justified, since filter extraction efficiencies are better than 95% [*Russell and Cass*, 1984].

The analytical detection limits for a 4-hour sample correspond to 4 neq m^{-3} for NO_3^-, SO_4^{2-}, HNO_3(g), and cations other than NH_4^+, and 8 neq m^{-3} for NH_4^+. Filter blanks for all constituents except Cl^- and NH_3(g) were below these detection limits. Because of substantial filter blanks, effective detection limits for NH_3(g) and Cl^- for a 4-hour sample were 17 neq m^{-3} and 20 neq m^{-3}, respectively.

Acknowledgments. We thank the organizations that provided us with sampling sites: California Air Resources Board, Western Oil and Gas Association, Buttonwillow Park and Recreation, Kern County Fire Department, and U.S. Army Corps of Engineers. We further thank the organizations who provided us with atmospheric data: West Side Operators, California Air Resources Board, National Weather Service, Getty Oil Company, Lemoore Naval Air Station, Tehachapi Fire Station, Edwards Air Force Base, and Kern County Air Pollution Control District. We express our gratitude to D. Buchholz and K. Mayer for their help in the field and to M. Lemons of Getty Oil Company (now Texaco) and the Boy Scouts of Lake Isabella for their contributions to the success of the sampling program. G. R. Cass and A. G. Russell (California Institute of Technology) provided many helpful discussions. This work was funded by the California Air Resources Board (contract A2-048-32). Correspondence should be addressed to M. R. Hoffmann.

REFERENCES

Aerovironment, Incorporated, AVKERN application report, *Rep. AV-FR-83/501R2*, Pasadena, Calif., 1984.

Appel, B. R., S. M. Wall, Y. Tokiwa, and M. Haik, Simultaneous nitric acid, particulate nitrate, and acidity measurements in ambient air, *Atmos. Environ.*, *14*, 549–554, 1980.

Bassett, M. E., and J. H. Seinfeld, Atmospheric equilibrium model of sulfate and nitrate aerosols, *Atmos. Environ.*, *17*, 2237–2252, 1983.

Boyce, S. D., and M. R. Hoffmann, Kinetics and mechanism of the formation of hydroxymethanesulfonic acid at low *p*H, *J. Phys. Chem.*, *88*, 4740–4746, 1984.

Brewer, R. L., E. C. Ellis, R. J. Gordon, and L. S. Shepard, Chemistry of mist and fog from the Los Angeles urban area, *Atmos. Environ.*, *17*, 2267–2271, 1983.

California Air Resources Board, Emission inventory 1979, report, Stationary Source Control Div., Emiss. Invent. Branch, Sacramento, 1982.

Calvert, J. G., and W. R. Stockwell, Mechanism and rates of the gas-phase oxidations of sulfur dioxide and nitrogen oxides in the atmosphere, in *Acid Precipitation: SO_2, NO, and NO_2 Oxidation Mechanisms: Atmospheric Considerations*, edited by J. G. Calvert, pp. 1–62, Butterworth, Woburn, Mass., 1984.

Cass, G. R., S. Gharib, M. Peterson, and J. W. Tilden, The origin of ammonia emissions to the atmosphere in an urban area, *Open File Rep. 82-6*, Environ. Qual. Lab., Calif. Inst. of Technol., Pasadena, 1982.

Cooper, J. A., and J. G. Watson, Jr., Receptor-oriented methods of air particulate source apportionment, *J. Air Pollut. Control Assoc.*, *30*, 1116–1125, 1980.

Crump, J. G., R. C. Flagan, and J. H. Seinfeld, An experimental study of the oxidation of sulfur dioxide in aqueous manganese sulfate aerosols, *Atmos. Environ.*, *17*, 1277–1289, 1983.

Damschen, D. E., and L. R. Martin, Aqueous aerosol oxidation of nitrous acid by O_2, O_3, and H_2O_2, *Atmos. Environ.*, *17*, 2005–2011, 1983.

Dasgupta, P. K., K. DeCesare, and J. C. Ullrey, Determination of atmospheric sulfur dioxide without tetrachlormercurate(II) and the mechanism of the Schiff reaction, *Anal. Chem.*, *52*, 1912–1922, 1980.

Davies, C. N., and M. Subari, Aspiration above wind velocity of aerosols with thin-walled nozzles facing and at right angles to the wind direction, *J. Aerosol Sci.*, *13*, 59–71, 1982.

Dionex Corporation, Determination of anions in acid rain, *Appl. Note 31*, Sunnyvale, Calif., 1981.

Dollard, G. J., and M. H. Unsworth, Field measurements of turbulent fluxes of wind-driven fog drops to a grass surface, *Atmos. Environ.*, *17*, 775–780, 1983.

Granett, A. L., and R. C. Musselman, Simulated acid fog injures lettuce, *Atmos. Environ.*, *18*, 887–891, 1984.

Heikes, B. G., and A. M. Thompson, Effects of heterogeneous processes on NO_3, HONO, and HNO_3 chemistry in the troposphere, *J. Geophys. Res.*, *88*, 10,883–10,896, 1983.

Hering, S. V., and D. L. Blumenthal, Fog sampler intercomparison study: Final report, Coord. Res. Counc., Atlanta, Ga., 1985.

Hoffmann, M. R., Comment on acid fog, *Environ. Sci. Technol.*, *18*, 61–64, 1984.

Hoffmann, M. R., and D. J. Jacob, Kinetics and mechanisms of the catalytic autoxidation of dissolved sulfur dioxide in aqueous solution: An application to nighttime fogwater chemistry, in *Acid Precipitation: SO_2, NO, and NO_2 Oxidation Mechanisms: Atmospheric Considerations*, edited by J. G. Calvert, pp. 101–172, Butterworth, Woburn, Mass., 1984.

Holets, S., and R. N. Swanson, High-inversion fog episodes in central California, *J. Appl. Meteorol.*, *20*, 890–899, 1981.

Huebert, B. J., Measurements of the dry-deposition flux of nitric acid vapor to grasslands and forest, in *Precipitation Scavenging, Dry Deposition, and Resuspension*, vol. 2, edited by H. R. Pruppacher, R. G. Semonin, and W. G. N. Slinn, pp. 785–794, Elsevier North-Holland, New York, 1983.

Jacob, D. J., The origins of inorganic acidity in fogs, Ph.D. thesis, Calif. Inst. of Technol., Pasadena, 1985.

Jacob, D. J., and M. R. Hoffmann, A dynamic model for the production of H^+, NO_3^-, and SO_4^{2-} in urban fog, *J. Geophys. Res.*, *88*, 6611–6621, 1983.

Jacob, D. J., J. M. Waldman, J. W. Munger, and M. R. Hoffmann, A field investigation of physical and chemical mechanisms affecting pollutant concentrations in fog droplets, *Tellus*, *36B*, 272–285, 1984*a*.

Jacob, D. J., R.-F. T. Wang, and R. C. Flagan, Fogwater collector design and characterization, *Environ. Sci. Technol.*, *18*, 827–833, 1984*b*.

Jacob, D. J., J. M. Waldman, J. W. Munger, and M. R. Hoffmann, Chemical composition of fogwater collected along the California coast, *Environ. Sci. Technol.*, *19*, 730–736, 1985.

Jacob, D. J., J. M. Waldman, J. W. Munger, and M. R. Hoffmann, The H_2SO_4-HNO_3-NH_3 system at high humidities and in fogs, 2, Comparison of field data with thermodynamic calculations, *J. Geophys. Res.*, this issue.

Kaplan, D. J., D. M. Himmelblau, and C. Kanaoka, Oxidation of sulfur dioxide in aqueous ammonium sulfate aerosols containing manganese as a catalyst, *Atmos. Environ.*, *15*, 763–773, 1981.

Katz, U., A droplet impactor to collect liquid water from laboratory clouds for chemical analysis, *Conf. Int. Phys. Nuages Commun., 8th*, 697–700, 1980.

Keene, W. C., J. N. Galloway, and J. D. Holden, Jr., Measurement of weak organic acidity in precipitation from remote areas of the world, *J. Geophys. Res.*, *88*, 5122–5130, 1983.

Martell, A. E., and R. M. Smith, *Critical Stability Constants*, vol. 3, Plenum, New York, 1977.

Martin, L. R., Kinetic studies of sulfite oxidation in aqueous solution, in *Acid Precipitation: SO_2, NO, and NO_2 Oxidation Mechanisms: Atmospheric Considerations*, edited by J. G. Calvert, pp. 63–100, Butterworth, Woburn, Mass., 1984.

Munger, J. W., D. J. Jacob, J. M. Waldman, and M. R. Hoffmann, Fogwater chemistry in an urban atmosphere, *J. Geophys. Res.*, *88*, 5109–5121, 1983.

Munger, J. W., D. J. Jacob, and M. R. Hoffmann, The occurrence of bisulfite-aldehyde addition products in fog and cloudwater, *J. Atmos. Chem.*, *1*, 335–350, 1984.

Reible, D. D., Investigations of transport in complex atmospheric flow systems, Ph.D. thesis, Calif. Inst. of Technol., Pasadena, 1982.

Russell, A. G., Analysis of oxalic acid impregnated filters for ammonia determination, *Open File Rep. 83-1*, Environ. Qual. Lab., Calif. Inst. of Technol., Pasadena, 1983.

Russell, A. G., and G. R. Cass, Acquisition of regional air quality model validation data for nitrate, sulfate, ammonium ion and their precursors, *Atmos. Environ.*, *18*, 1815–1827, 1984.

Scherbatskoy, T., and R. M. Klein, Response of spruce and birch foliage to leaching by acidic mists, *J. Environ. Qual.*, *12*, 189–195, 1983.

Schwartz, S. E., and W. H. White, Solubility equilibria of the nitrogen oxides and oxyacids in dilute aqueous solution, *Adv. Environ. Sci. Eng.*, *4*, 1–45, 1981.

Sehmel, G. A., Particle and gas dry deposition: A review, *Atmos. Environ.*, *14*, 983–1011, 1980.

Slinn, W. G. N., Predictions for particle deposition on vegetative canopies, *Atmos. Environ.*, *16*, 1785–1794, 1982.

Smith, R. M., and A. E. Martell, *Critical Stability Constants*, vol. 4, Plenum, New York, 1976.

Sørensen, P. E., and V. S. Andersen, The formaldehyde-hydrogen sulphite system in alkaline aqueous solution: Kinetics, mechanisms, and equilibria, *Acta Chem. Scand.*, *24*, 1301–1306, 1970.

Spicer, C. W., and P. M. Schumacher, Particulate nitrate: Laboratory and field studies of major sampling interferences, *Atmos. Environ.*, *13*, 543–552, 1979.

Spicer, C. W., J. E. Howes, T. A. Bishop, and L. H. Arnold, Nitric acid measurement methods: An intercomparison, *Atmos. Environ.*, *16*, 1487–1500, 1982.

Stelson, A. W., and J. H. Seinfeld, Relative humidity and temperature dependence of the ammonium nitrate dissociation constant, *Atmos. Environ.*, *16*, 983–992, 1982.

Stumm, W., and J. J. Morgan, *Aquatic Chemistry*, pp. 129–132, Wiley-Interscience, New York, 1970.

Waldman, J. M., Depositional aspects of pollutant behavior in fog, Ph.D. thesis, Calif. Inst. of Technol., Pasadena, 1986.

Waldman, J. M., J. W. Munger, D. J. Jacob, and M. R. Hoffmann, Chemical characterization of stratus cloudwater and its role as a vector for pollutant deposition in a Los Angeles pine forest, *Tellus*, *37*, 91–108, 1985.

Weast, R. C. (Ed.), *Handbook of Chemistry and Physics*, 65th ed., Chemical Rubber Company, Cleveland, Ohio, 1984.

D. J. Jacob, Center for Earth and Planetary Physics, Harvard University, Cambridge, MA 02138.

M. R. Hoffmann, J. W. Munger, and J. M. Waldman, Environmental Engineering Science, W. M. Keck Engineering Laboratories, California Institute of Technology, Pasadena, CA 91125.

(Received February 15, 1985;
revised July 25, 1985;
accepted July 31, 1985.)